Quantitative residue-specific protein backbone torsion angle dynamics from concerted measurement of ^{3}J couplings

Jung Ho Lee, Fang Li, Alexander Grishaev, and Ad Bax

Laboratory of Chemical Physics, National Institute of Diabetes and Digestive and Kidney Diseases, National Institutes of Health, Bethesda, MD 20892, USA

SUPPORTING INFORMATION

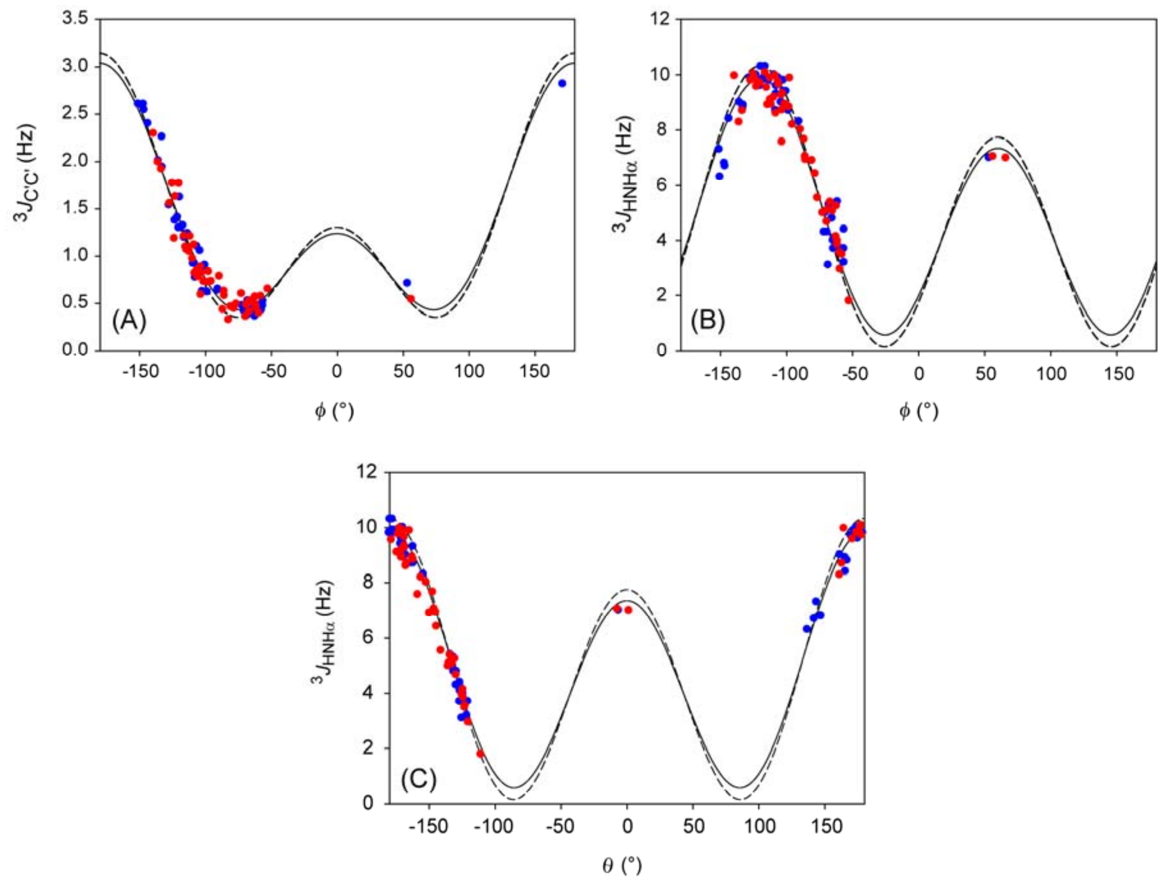

Figure S1. Plots of experimental (A) $^3J_{C'C'}$ and (B) $^3J_{HNH\alpha}$ values against the backbone torsion angle ϕ, superimposed on the best-fit Karplus equations $^3J_{C'C'} = 1.61 \times \cos^2\phi - 0.93 \times \cos\phi + 0.55$ and $^3J_{HNH\alpha} = 7.97 \times \cos^2(\phi\text{-}60) - 1.26 \times \cos(\phi - 60) + 0.63$ (solid lines). The dashed lines represent the Karplus curve after factoring out the effect of motion, c.f. eq 2 ($\sigma = 0.226$), and correspond to the coefficients listed in Table 1, main text. Blue data points correspond to ϕ angles extracted from the RDC-refined GB3 structure (refined without $^3J_{C'C'}$ and $^3J_{HNH\alpha}$ data[1]); red data points correspond to the RDC-refined ubiquitin structure (PDB entry 2MJB). Residues with elevated backbone dynamics (L12, D40, and G41 for GB3; T7-K11, D32-G35, A46, G47, D52, and V70-G76 for ubiquitin) are excluded from the plots. (C) Plot of $^3J_{HNH\alpha}$ values measured for GB3 (blue) and ubiquitin (red) against the H-N-C$^\alpha$-H$^\alpha$ dihedral angle, θ (Note: $\theta \approx \phi$ - 60º). The solid and dashed line represent the best-fit and dynamics-factored-out ($\sigma = 0.226$) Karplus curves, respectively. The rmsd values between observed and best-fitted $^3J_{HNH\alpha}$ values are 0.34 and 0.69 Hz for GB3 when using H-N-C$^\alpha$-H$^\alpha$ dihedral angle (θ) and torsion angle (ϕ - 60º), respectively, and the corresponding values are 0.43 and 0.61 Hz for ubiquitin.

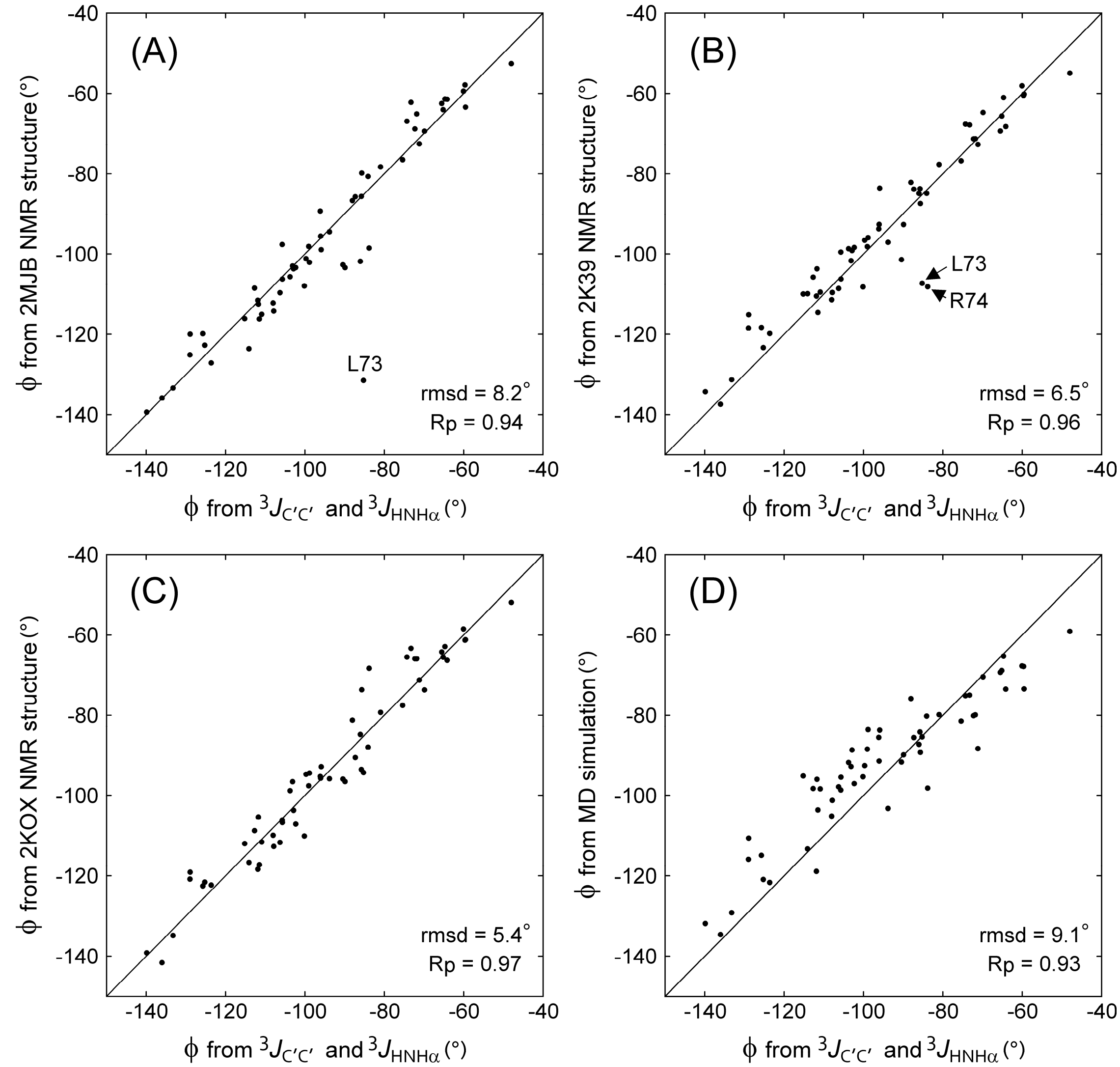

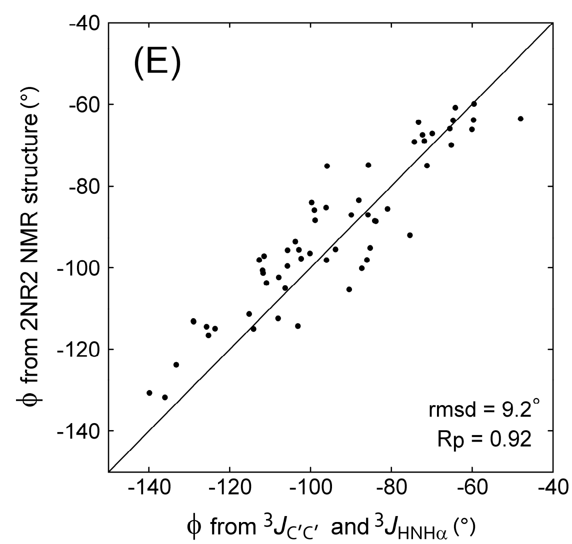

SI Figure S2. Comparison of <ϕ> values extracted from Fig. 1A with averaged <ϕ> values from (A) the single model, RDC-refined NMR structure (PDB entry 2MJB), (B) PDB ensemble 2K39,[2] (C) PDB ensemble 2KOX,[3] (D) a 1-ms molecular dynamics trajectory,[4] and (E) PDB ensemble 2NR2.[5] Only ensemble conformers with $\phi < 0°$ were included in calculating <ϕ>.

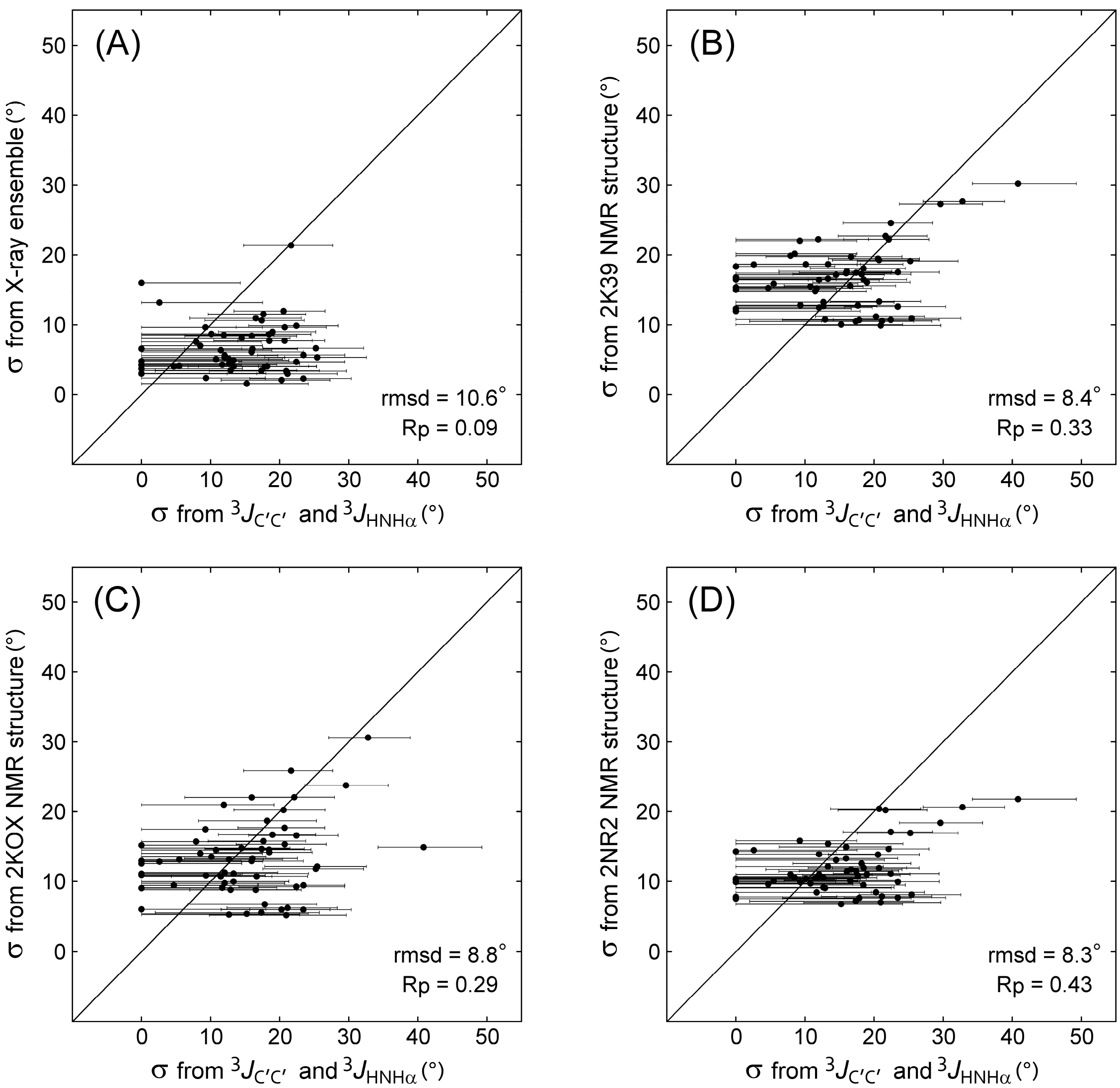

SI Figure S3. Comparison of σ values extracted from Fig. 1A with ϕ standard deviations in various ubiquitin ensembles: (A) a set of 15 high-resolution (≤ 1.8 Å) X-ray structures, listed in the SI of Maltsev et al.[6]; (B) PDB entry 2K39,[2] (C) PDB entry 2KOX,[3] (D) PDB entry 2NR2.[5] Only ensemble conformers with $\phi < 0°$ were included for calculating σ.

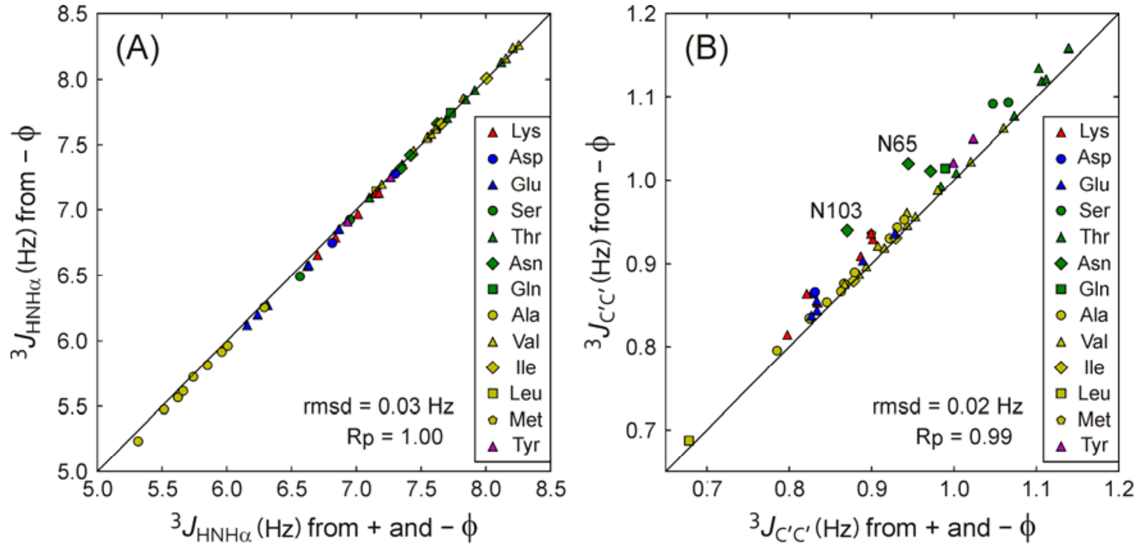

Figure S4. Effect of ignoring conformers with positive ϕ angles on calculated ^{3}J couplings for the α-synuclein ensemble derived by Mantsyzov et al.[8] (A) $^3J_{HNH\alpha}$ and (B) $^3J_{C'C'}$ values calculated using only conformers with negative ϕ angles (y axis) versus values calculated for all conformers. The Karplus curve parameterization of Table 1 (σ=0°) was used for each individual conformer.

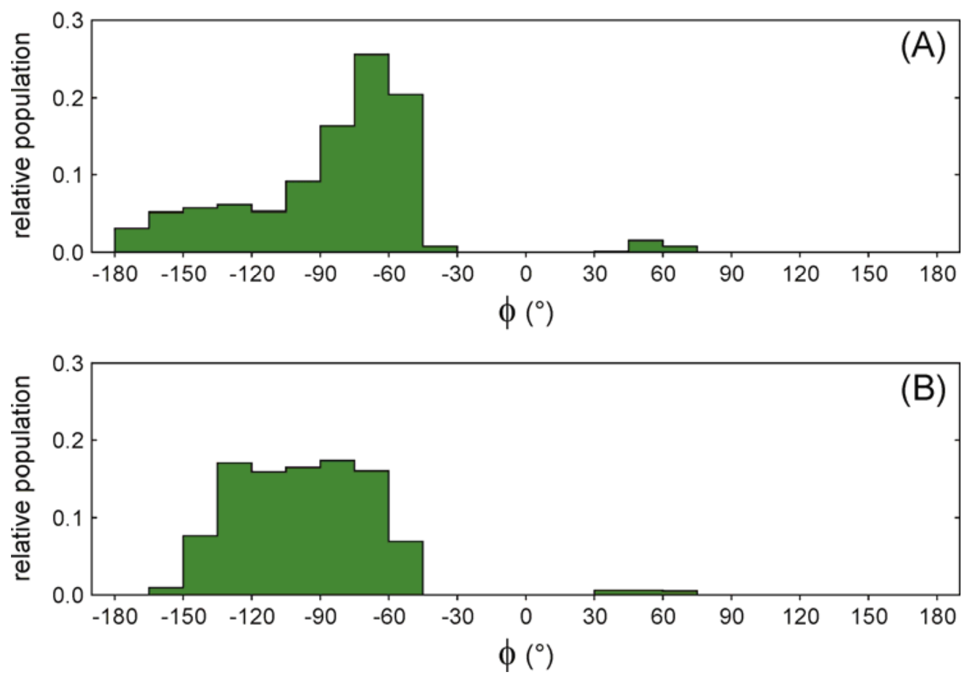

Figure S5. Backbone ϕ angle distribution sampled by (A) 9 Ala and (B) 11 Val residues of α-synuclein for which a complete set of NMR data was available to derive ϕ/ψ distributions by means of a maximum entropy approach.[8]

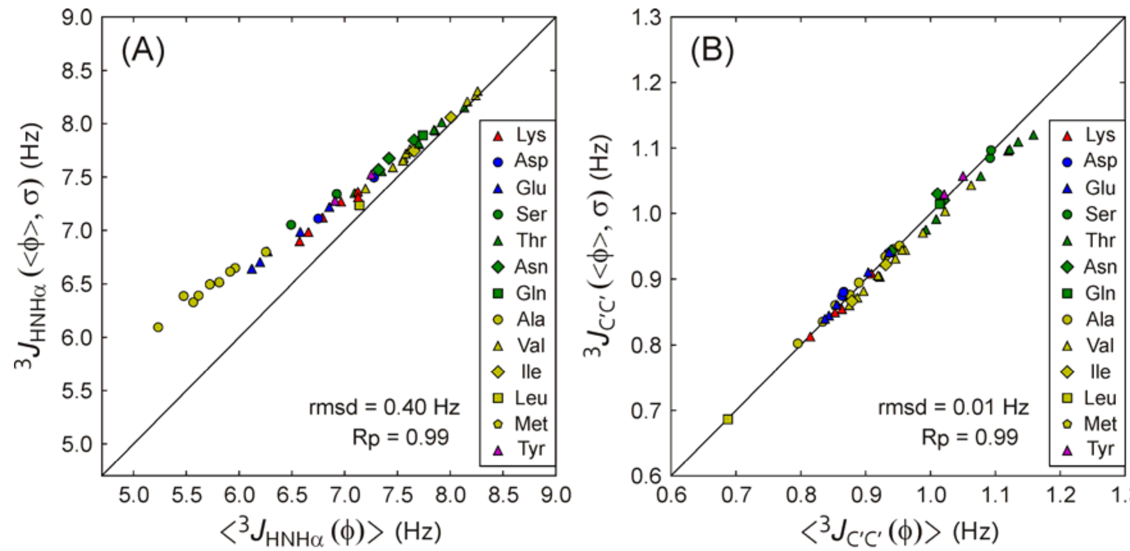

Figure S6. Impact of the Gaussian distribution approximation on predicted $^3J_{HNH\alpha}$ and $^3J_{C'C'}$ couplings in α-synuclein. For each residue in the α-synuclein ensemble of Mantsyzov et al.,[8] the x-axis corresponds to the (A) $^3J_{HNH\alpha}$ and (B) $^3J_{C'C'}$ coupling, calculated as the weighted average over $\phi < 0°$ conformers, using the Karplus parameters of Table 1 (σ=0°). The y-axis corresponds to the values calculated using $^3J = A' \cos^2\theta + B' \cos\theta + C'$, with A', B', and C' given by eq 2, where σ is calculated from the ensemble of Mantsyzov et al. while taking only conformers with $\phi < 0°$ into account when deriving <ϕ> and the standard deviation, σ. For $^3J_{HNH\alpha}$, $\theta = \phi - 60°$ is used.

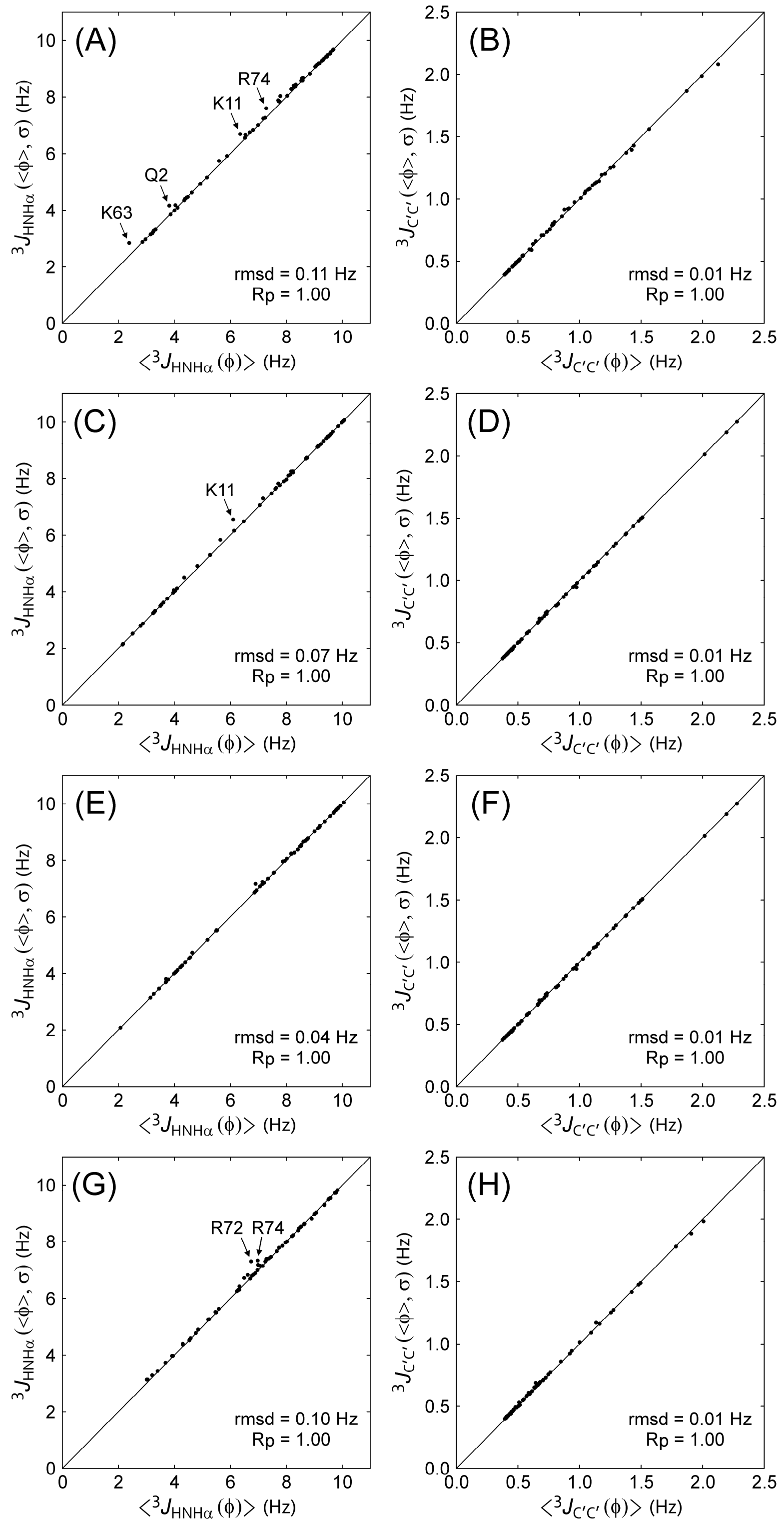

Figure S7. Impact of the Gaussian distribution approximation on predicted $^3J_{HNH\alpha}$ and $^3J_{C'C'}$ couplings in ubiquitin. The correlation plots for $^3J_{HNH\alpha}$ and $^3J_{C'C'}$ couplings, as described in the legend of Fig. S6, are shown for (A, B) PDB entry 2K39,[2] (C, D) PDB entry 2KOX,[3] (E, F) PDB entry 2NR2,[5] and (G, H) a 1-ms molecular dynamics trajectory.[4]

Table S1. σ and <ϕ> values derived from experimental $^{3}J_{C'C'}$ and $^{3}J_{HNH\alpha}$ values. [a]

Ubiquitin [b]	<ϕ> (°)	σ (°)	σ lower bound (°)	σ upper bound (°)
Q2	-96	18	10	24
I3	-133	22	14	29
F4	-114	12	0	20
V5	-129	12	0	21
K6	-102	18	11	25
T7	-99	12	0	19
L8	-65	3	0	18
T9	-96	0	0	14
K11	-86	22	15	28
T12	-111	14	0	21
I13	-113	9	0	17
T14	-103	10	0	18
L15	-124	13	0	21
E16	-106	0	0	15
V17	-140	0	0	0
E18	-115	8	0	17
D21	-71	25	18	33
T22	-88	0	0	15
N25	-72	18	7	25
V26	-73	23	16	30
K27	-65	15	0	24
A28	-66	17	2	26
K29	-72	21	12	28
I30	-74	20	12	27
Q31	-60	21	10	30
D32	-60	13	0	23
K33	-86	17	7	23
E34	-111	23	17	29
I36	-87	21	14	27
D39	-70	5	0	18
Q40	-100	11	0	18
Q41	-90	16	6	22
R42	-125	16	0	23
L43	-106	16	6	23
I44	-129	5	0	17
F45	-136	25	18	32
A46	41	16	0	32
K48	-112	22	16	28
Q49	-81	13	0	20
L50	-86	19	11	25
E51	-96	21	14	27

R54	-103	9	0	17
T55	-104	0	0	14
L56	-60	0	0	18
D58	-64	13	0	22
Y59	-99	11	0	19
N60	59	18	0	25
I61	-84	12	0	20
Q62	-108	21	13	27
K63	-48	13	0	24
S65	-75	18	8	25
T66	-112	9	0	18
L67	-106	0	0	15
H68	-108	18	10	25
L69	-100	17	9	24
V70	-126	17	4	24
L71	-90	22	16	28
R72	-94	33	27	39
L73	-85	30	24	36
R74	-84	41	34	49

GB3 [c]	<ϕ> (°)	σ (°)	σ lower bound (°)	σ upper bound (°)
Y3	-117	13	0	21
K4	-117	13	0	21
L5	-116	16	4	23
V6	-107	2	0	15
I7	-103	0	0	14
N8	-112	9	0	18
K10	-72	13	0	22
T11	-115	0	0	15
L12	-106	32	26	38
K13	-123	12	0	20
E15	-145	11	0	21
T16	-155	21	12	28
T17	-135	17	3	25
T18	-155	24	16	31
K19	-105	12	0	19
A20	-152	15	0	23
A23	-61	0	0	18
E24	-65	12	0	21
K28	-64	10	0	21
A29	-70	20	11	28
F30	-71	11	0	20
K31	-66	9	0	20

Q32	-74	21	12	28
Y33	-59	16	0	25
A34	-63	14	0	23
N35	-62	17	0	26
V39	-108	20	12	26
D40	-143	15	0	23
V42	-96	7	0	16
W43	-103	19	12	25
T44	-134	20	10	27
Y45	-141	12	0	21
D46	-115	13	0	21
D47	-67	0	0	17
A48	-67	10	0	20
T49	-108	0	0	15
K50	44	7	0	25
T51	-126	0	0	16
F52	-100	0	0	14
T53	-120	15	0	22
V54	-119	11	0	19
T55	-118	12	0	20

[a] ($^3J_{C'C'}$, $^3J_{HNH\alpha}$) values that lie outside $\sigma = 0$ in Fig. 1 were set to $\sigma = 0$.
[b] $^3J_{C'C'}$ values are measured with $^{13}C/^{15}N$-enriched ubiquitin sample at pH 6.6, 298 K and 500 MHz ^1H frequency. $^3J_{HNH\alpha}$ values are from Maltsev et al.[6]
[c] $^3J_{C'C'}$ values are from Li et al.[1]; $^3J_{HNH\alpha}$ values are from Vogeli et al.[7]

Table S2. $^3J_{C'C'}$ and $^3J_{HNH\alpha}$ couplings in α-synuclein, together with σ and <φ> values derived using the graphic analysis of Fig. 3.[a]

	<φ> (°)	σ (°)	σ lower bound (°)	σ upper bound (°)	$^3J_{C'C'}$ (Hz)	$^3J_{HNH\alpha}$ (Hz)
D2					0.80	
V3	-91	25	21	29	0.76	7.25
F4	-89	24	19	28	0.71	7.13
M5	-92	28	24	32	0.83	7.13
K6	-82	29	24	34	0.72	6.11
G7					0.66	
L8	-88	24	19	28	0.70	7.01
S9	-87	32	27	36	0.83	6.53
A17	-76	33	27	38	0.75	5.45
A18	-73	34	29	41	0.76	5.22
A19	-74	32	26	38	0.72	5.28
E20	-81	26	21	31	0.66	6.13
K21	-86	29	24	33	0.76	6.53
T22	-91	29	25	33	0.83	6.99
V26	-92	29	25	33	0.86	7.12
A27	-77	30	24	35	0.70	5.58
G31					0.71	
K32	-91	30	25	34	0.85	7.01
V37	-95	27	23	31	0.86	7.50
L38	-89	25	20	29	0.73	7.04
Y39	-98	30	26	34	0.97	7.47
V40	-106	30	26	33	1.15	8.01
G41					0.83	
A53	-79	30	25	35	0.72	5.79
A56	-77	31	26	36	0.73	5.61
E57	-82	29	24	33	0.71	6.15
K58	-87	31	27	36	0.83	6.57
T59	-91	28	24	33	0.82	7.01
N65	-98	29	26	33	0.96	7.51
V66	-96	30	26	34	0.92	7.34
G67					0.75	
A69	-79	30	25	35	0.72	5.83
V70	-95	27	22	31	0.86	7.53
V71	-106	28	24	32	1.11	8.15
T72	-101	30	26	33	1.02	7.70
T75	-98	28	24	32	0.94	7.62
A76	-80	33	28	39	0.80	5.87
V77	-96	29	25	33	0.92	7.45
A78	-77	30	25	36	0.71	5.62
Q79	-89	30	25	34	0.82	6.79

K80	-89	31	27	35	0.84	6.71
T81	-97	29	25	33	0.93	7.52
V82	-99	29	25	33	0.97	7.65
E83	-83	31	26	36	0.77	6.19
G84					0.80	
A85	-77	30	25	35	0.70	5.64
G86					0.72	
S87	-92	33	29	38	0.93	6.82
I88	-95	28	24	32	0.89	7.46
F94	-93	33	29	37	0.93	6.92
D98	-86	26	21	31	0.72	6.72
Q99	-94	30	25	34	0.89	7.23
L100	-87	25	21	30	0.71	6.80
G101					0.70	
K102	-91	32	28	37	0.90	6.83
N103	-93	29	25	33	0.87	7.20
G106					0.77	
Q109	-92	31	27	35	0.89	6.94
E110	-87	32	27	36	0.83	6.52
D115	-90	30	25	34	0.83	6.85
V118	-98	28	24	32	0.95	7.68
E123	-85	27	23	32	0.73	6.55
A124	-83	30	25	35	0.76	6.23
S129	-90	34	30	39	0.92	6.65
Y133	-92	34	30	39	0.95	6.77
Q134	-104	33	30	37	1.14	7.55
E139	-86	26	22	31	0.72	6.71

[a] Derived from $^3J_{C'C'}$ values, measured for a $^{13}C/^{15}N$-enriched α-synuclein sample at pH 6.0, 288 K and 600 MHz ^1H frequency. $^3J_{HNH\alpha}$ values are from Mantsyzov et al.[8]

References

1. Li, F.; Lee, J. H.; Grishaev, A.; Ying, J.; Bax, A., *ChemPhysChem* **2014,** http://dx.doi.org/10.1002/cphc.201402704 .
2. Lange, O. F.; Lakomek, N. A.; Fares, C.; Schroder, G. F.; Walter, K. F. A.; Becker, S.; Meiler, J.; Grubmuller, H.; Griesinger, C.; de Groot, B. L., *Science* **2008,** 320, 1471-1475.
3. Fenwick, R. B.; Esteban-Martin, S.; Richter, B.; Lee, D.; Walter, K. F. A.; Milovanovic, D.; Becker, S.; Lakomek, N. A.; Griesinger, C.; Salvatella, X., *J. Am. Chem. Soc.* **2011,** 133, 10336-10339.
4. Piana, S.; Lindorff-Larsen, K.; Shaw, D. E., *Proc. Natl. Acad. Sci. U. S. A.* **2013,** 110, 5915-5920.
5. Richter, B.; Gsponer, J.; Varnai, P.; Salvatella, X.; Vendruscolo, M., *J. Biomol. NMR* **2007,** 37, 117-135.
6. Maltsev, A. S.; Grishaev, A.; Roche, J.; Zasloff, M.; Bax, A., *J. Am. Chem. Soc.* **2014,** 136, 3752-3755.
7. Vogeli, B.; Ying, J. F.; Grishaev, A.; Bax, A., *J. Am. Chem. Soc.* **2007,** 129, 9377-9385.
8. Mantsyzov, A. B.; Maltsev, A. S.; Ying, J.; Shen, Y.; Hummer, G.; Bax, A., *Protein Sci.* **2014,** 23, 1275-90.